Photochemical & Photobiological Sciences

PAPER

View Article Online
View Journal

Cite this: DOI: 10.1039/c7pp00448f

1,2,4,5-Benzenetetracarboxylic acid: a versatile hydrogen bonding template for controlling the regioselective topochemical synthesis of head-to-tail photodimers from stilbazole derivatives†

Gabriela Ortega,[a] Jesús Hernández,[a] Teresa González,[a] Romano Dorta[b] and Alexander Briceño*[a]

The crystal engineering of hydrogen bonded organic assemblies based on 1,2,4,5-benzenetetracarboxylic acid (H_4bta) and stilbazole derivatives (**1–10**) is exploited to provide regio-controlled [2 + 2] photocycloadditions in the solid state. Single crystal X-ray diffraction analyses have revealed that all the arrays are built-up from the self-assembly of the $(H_2bta)^{2-}$ dianion with two stilbazolium cations *via* O–H···O$^-$ and N$^+$–H···O$^-$ charge-assisted H-bonding synthons: (4-Hstilbazolium$^+$)$_2$(H_2bta^{2-}). The dianion displays an interesting diversity of H-bonding motifs. Such structural flexibility allowed us to obtain four structure-types defined by the preferential formation of intramolecular or intermolecular hydrogen bonds between carboxylate-carboxylic groups. In these ionic assemblies two predominant structural H-bonding patterns were observed. The first pattern is characterised by the formation of intramolecular H-bonds in the dianion, leading to discrete assemblies based on ternary arrays. The second hydrogen pattern consists of 2-D hydrogen networks built-up from the self-assembly of anions *via* intermolecular H-bonds that are linked to the cations. Two additional examples, in which the dianion is self-assembled in two types of ribbons, were also observed. Another supramolecular feature predominant in all these arrays is the stacking of the cations in a *head-to-tail* fashion, which is controlled *via* cation–π interactions. These arrays are photoactive in the solid state upon UV-irradiation leading to the regioselective synthesis of *rctt*-cyclobutane *head-to-tail*-isomers in high to quantitative yield. In this work, the template tolerance either to steric or electronic effects by changing the number or positions of the supramolecular interactions exerted by distinctive functional groups was also explored. In addition, assemblies bearing 2-chloro (**7** and **8**) and 3-chloro-4-stilbazole (**1** and **9**) crystallize in two different crystalline forms, leading to novel examples of supramolecular isomers with similar solid state reactivity.

Received 12th December 2017,
Accepted 26th March 2018

DOI: 10.1039/c7pp00448f

rsc.li/pps

Introduction

In recent times, supramolecular assistance has emerged as an efficient approach of controlling reactivity in the solid state.[1–3] The use of auxiliary molecules as templates in synthesis is now a well-recognised approach for the preparation of a wide variety of molecular and supramolecular arrangements. In particular, hydrogen bonding templates[1] and metal-templated assemblies[2] extended to multivalent templates[3] have been employed successfully for topochemical [2 + 2] photodimerisations. More recently, the use of ionic interactions has become an important tool as an alternative synthetic approach to prepare stereocontrolled compounds either in solution or in the solid state.[4–7] In particular, Yamada and Ramamurthy's groups have reported a very strong and reliable effect of protonated unsaturated pyridyl compounds in a supramolecular approach to orient molecules in a parallel fashion.[5,6]

In general, this methodology can be used to steer the self-assembly of novel photoactive arrangements based on asymmetrical olefins with enforced *head-to-tail* stacking. The preferential obtaining of this configuration is a direct consequence of strong pyridinium–π interactions.[5,6] The strength of these

[a]*Laboratorio de Síntesis y Caracterización de Nuevos Materiales, Centro de Química, Instituto Venezolano de Investigaciones Científicas, San Antonio de Los Altos, Miranda, Venezuela. E-mail: abriceno@ivic.gob.ve; Fax: +58-212-5041350; Tel: +58-212-5041320*

[b]*Department Chemie und Pharmazie, Anorganische und Allgemeine Chemie, Friedrich–Alexander–Universität Erlangen–Nürnberg, Egerlandstr. 1, 91058 Erlangen, Germany*

† Electronic supplementary information (ESI) available: Experimental characterization (m.p and EA) and FT-IR spectra of compounds **1–10**. ^{1}H-NMR spectra of stilbazoles and photophoducts. Powder X-Ray Diffraction data of the ionic assemblies. CCDC 1447029–1447039. For ESI and crystallographic data in CIF or other electronic format see DOI: 10.1039/c7pp00448f

interactions can be tuned by varying the π-electron density on the aryl rings through the attached substituents. More recently, Vittal and co-workers also have reported examples of solid state reactivity of ionic assemblies based on unsaturated carboxylic acids and molecules bearing pyridyl groups.[7] Although electrostatic interactions are less directional in comparison to other supramolecular interactions such as coordination bonds or hydrogen bonds, such interactions can nevertheless be used for a rational design of molecular assemblies. This makes it a challenge to predict the relative orientations of ionic counterparts in organic molecular salts when compared to neutral co-crystals. We have anticipated that a simple manner to modulate the directionality of ionic interactions is to use robust charge-assisted hydrogen bonds in self-assemblies directed by charge-assisted carboxylate–pyridinium hydrogen bonding synthons.[8] In this context, as part of our ongoing efforts to design and prepare photoreactive solids, we have been able to engineer novel photoreactive multicomponent assemblies based on the modular self-assembly of carboxylic acid and unsaturated stilbene and stilbazole derivatives.[9]

Inspired by Shan and Jones's work,[10] we recognised the potential of 1,2,4,5-benzenetetracarboxylic acid (H_4bta) as an interesting multivalent template to act as an H-bonding supramolecular switch, which could be used to organize novel photoactive arrangements based on asymmetrical olefins with enforced *head-to-tail* stacking (Scheme 1). In particular, the presence of pyridyl or amine groups leads to ionic multicomponent assemblies due to proton transfer between them.[11] We have demonstrated that it is possible to induce the transformation of the H_4bta molecule from a homotopic into a flexible heterotopic template[9a] (presence either of carboxylate or carboxylic groups). Thus, deprotonated partial form of the H_4bta can act either as hydrogen bond acceptor or hydrogen bond donor, leading to new supramolecular arrays in combination with N-heterocyclic targets. Herein, we extend the use of this template as a versatile supramolecular switch to modulate from molecular to supramolecular ionic assemblies with a wide variety of asymmetrical olefins. In this contribution, we evaluate a set of stilbazole derivatives displaying halogen (–Cl or –Br) and bulky substituents (–CN), which thanks to different substituents on the aryl ring exert distinctive steric and electronic demands together with possible side interaction forces in the supramolecular ionic assemblies (Scheme 2). Thus, directing effects and relative contributions of such substituents on steric, cation–π, and halogen···halogen interactions were observed. We report the successful extension of this approach to the assembly of ten novel photoactive ionic arrangements based on H_4bta and stilbazole derivatives (Scheme 1): (3-Cl-Hstb$^+$)$_2$(H_2bta^{2-}) (**1**), (2,4-di-Cl-Hstb$^+$)$_2$ (H_2bta^{2-}) (**2**), (3-Br-Hstb$^+$)$_2$ (H_2bta^{2-}) (**3**), (4-Br-Hstb$^+$)$_2$(H_2bta^{2-}) (**4**) (3-CN-Hstb$^+$)$_2$(H_2bta^{2-}) (**5**), (2-CN-Hstb$^+$)$_2$(H_2bta^{2-}) (**6**), (2-Cl-Hstb$^+$)$_2$(H_2bta^{2-}) (**7**), (2-Cl-Hstb$^+$)$_2$ (H_2bta^{2-}) (**8**) (3-Cl-Hstb$^+$)$_2$(H_2bta^{2-}) (**9**) and (4-CN-Hstb$^+$)$_2$(H_2bta^{2-}) (**10**).

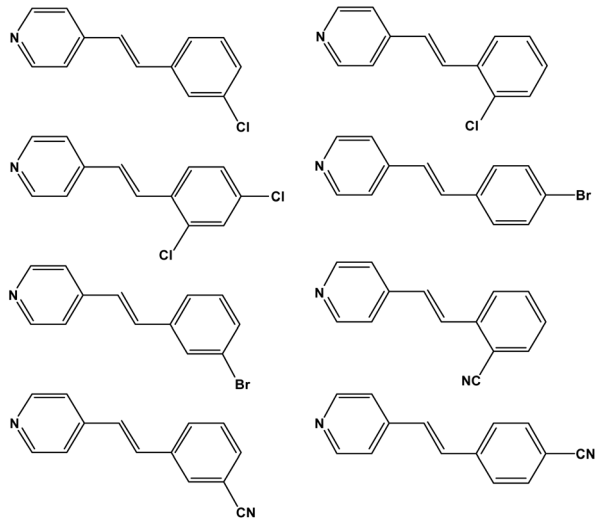

Scheme 2 Structure diagram of stilbazole molecules used for the synthesis of ionic assemblies.

All the arrays are photoreactive in the solid state upon UV-irradiation, leading to the regioselective synthesis of *rctt-head-to-tail*-photodimers. In addition, assemblies bearing 2-chloro- (**7** and **8**) and 3-chloro-4-stilbazole (**1** and **9**) crystallize in two different forms, resulting in two new examples of supramolecular isomers[12] with similar solid state reactivity.

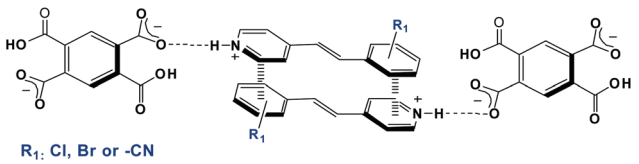

Scheme 1 Schematic representation of H-bonded assemblies directed by charge-assisted hydrogen bonds between cations and anions, showing cation–π interactions.

Experimental

All chemicals and solvents were purchased from Aldrich and were used as received without further purification. The FT-IR spectra were recorded from KBr pellets in the range 4000–400 cm^{-1} on a Thermo-Scientific FT/IR spectrometer. The C, H and N elemental analyses were conducted on a Fisons-EA1108 CHNS-O elemental analyzer. 1H-NMR spectra were recorded on Bruker 300 and 500 MHz spectrometers from solution in d_6-DMSO solutions.

X-Ray crystallography

Single crystal X-ray diffraction. Suitable single crystals of compounds **1–11** were mounted on a glass fiber and data sets were collected at 298(2) K on a Rigaku diffractometer, AFC-7, Mercury CCD-detector, Mo-Kα (λ = 0.71073 Å) radiation. Data collection was performed using φ and ω scans. Non-hydrogen atoms were located from the difference E-maps by means of direct methods and the structural data were refined by full-

matrix least-squares methods on F^2 using the *SHELXL-2013* crystallographic software package.[13] Anisotropic thermal parameters were used to refine all non-hydrogen atoms. The H atoms on the C atoms were included in calculated positions. The H-atoms on carboxylic groups were located from Fourier maps. The powder X-ray diffraction (PXRD) patterns were collected on a Siemens D5005 X-ray diffractometer with Bragg–Brentano geometry, using a zero background sample holder (Si (510) single crystal) and Cu Kα (1.5418 Å) and operated at 40 kV–30 mA.

General procedure

Methods for obtaining single crystals between stilbazole derivatives and 1,2,3,4-benzenetetracarboxylic acid (H_4bta). Crystals of all H-bonded assemblies were prepared by mixing H_4bta (100 mg, 0.4 mmol) and the respective stilbazole compound (0.8 mmol), previously dissolved in a MeOH–DMSO mixture in a 1 : 1 vol/vol ratio with a final volume of 30 mL. Some trials were made only in methanol as solvent for example the preparation of assemblies bearing 2-Cl-4-Stb and 3-Cl-4-Stb. The resulting solutions were left to evaporate at room temperature until crystals appeared. The crystals were removed from the solution before complete evaporation in order to obtain good quality single crystal. The experimental data for each ionic assembly are shown in Table 1 (See ESI†). The PXRD patterns reveal that such phases are obtained with a high crystalline purity for the majority of the phases, except for the polymorphs of 2-Cl-4-Stb (**7–8**) and 3-Cl-4-Stb (**1**) (See ESI†).

Results and discussion

The combination of H_4bta with 2 molar equiv. of stilbazole derivatives in solution gave crystals of **1–10**. All the assemblies were characterised by elemental analysis, FT-IR and single crystal X-ray studies. The relative molar ratios of both components were established by elemental analyses and subsequently confirmed by crystal structure determinations. As expected, all the crystals formed 2 : 1 anhydrous stilbazolium/dicarboxylate assemblies. Solid state FT-IR spectroscopy confirmed the proton transfer from H_4bta to the stilbazole molecule in each structure, which is reflected by a reduction in the relative intensity of the carboxyl C═O stretching mode between the range 1708 and 1687 cm^{-1} in comparison to the starting acid. Additionally, the appearance of two strong absorption bands in the range of 1628 and 1336 cm^{-1} is characteristic of the carboxylate groups due to the asymmetric and symmetric C–O stretching modes, respectively, and a third broad band between 2160 and 2134 cm^{-1} is assigned to the O···H–N interactions of the stilbazolium cations.

Description of crystal structures (1–10)

Single crystal X-ray diffraction analyses of all the structures showed a common structural feature: the deprotonation of two acids of the four –COOH groups in H_4bta is revealed by C–O distances in the range of 1.210–1.266 Å in the carboxylate anions, whereas the C–O and C═O bond lengths in the free carboxylic acid functions display typical distances in the range of 1.296–1.324 Å and 1.203–1.234 Å, respectively. In addition, all asymmetric units of structures **1–10** contain a cation in a general position and half a $(H_2bta)^{2-}$ dianion lying about an inversion centre, and the arrays are built-up from the self-assembly of a $(H_2bta)^{2-}$ dianion with two stilbazolium cations *via* O–H···O^- and N^+–H···O^- charge-assisted hydrogen bonds. In particular, cation–anion interactions are directed by the formation of carboxylate–pyridinium hydrogen bonding synthons of type II and III (Scheme 3).

The dianion displays an interesting diversity of H-bonding motifs, and this structural flexibility generates four structure types described by the preferential formation of intra- or intermolecular hydrogen bonds between carboxylate and carboxylic acid groups. In the ionic assemblies described here two structural patterns are predominant. The first is characterised by the formation of O–H···O^- charge-assisted intramolecular H-bonds in the dianion, leading to discrete assemblies based on ternary arrays, *i.e.* $(4\text{-HStilbazolium}^+)_2(H_2bta^{2-})$ The second structure type consists of 2-D hydrogen bonding networks built-up from the self-assembly of anions *via* O–H···O^- intermolecular H-bonds between carboxylic acid and carboxylate groups. These layers are linked by the cations. Two additional examples, in which the dianion is self-assembled in two types of ribbons, were also observed.

Formation of discrete ionic assemblies directed by O–H···O^- and N^+–H···O^- charge-assisted hydrogen bonds. Crystal structures of ionic assemblies 1–5

Hydrogen-bonded assemblies **1–5** crystallise in triclinic system with $P\bar{1}$ space group and related unit cell parameters. Details are summarised in Table 1. The asymmetric units contain one stilbazolium cation $(4\text{-Hstb})^+$ in a general position and half of a $(H_2bta)^{2-}$ dianion located on a special position 1*a* (0,0,0). Each anion forms two O–H···O^- intramolecular H-bonds between carboxylic–carboxylate groups, leading to a quasi-planar molecular motif. Further, the anion is linked to two cations *via* N^+–H···O^- H-bonds, forming a ring with additional C–H···O interactions described by the graph symbol $R^2_2(7)$ (heterosynthon type II).[14] Such interactions generate a centrosymmetric discrete supramolecular ionic assembly with the general formula $(n\text{-}R_1\text{-Hstb}^+)_2(H_2bta^{2-})$ where *n*: 2, 3 or 4 and R_1: Cl, Br or –CN (Details of geometrical parameters of charge-assisted H-bonds are shown in Table 2). Thus, the ternary supramolecular motif is self-assembled into supramolecular ribbons directed by cation–π interactions between pyridinium and aryl rings with distance in the range of 3.81–4.29 Å (Fig. 1 (a–e)). In these structures, depending on the number or position of the distinctive ring substituents, some structural differences and supramolecular interactions exerted by these functional groups were observed. In structure $(3\text{-Cl-Hstb}^+)_2(H_2bta^{2-})$ (**1**) the cation–π interaction occurs between ternary assemblies located in different supramolecular 1D-arrays without cation–cation interactions in this direction (Fig. 1(a)). In structures $(2,4\text{-di-Cl-Hstb}^+)_2(H_2bta^{2-})$ (**2**) and 2(3-

Table 1 Crystal data, data collection and structure refinement for compounds **1–11**

	(3-Cl-Hstb$^+$)$_2$(H$_2$bta^{2-}) (**1**)	(2,4-di-Cl-Hstb$^+$)$_2$(H$_2$bta^{2-}) (**2**)	(3-Br-Hstb$^+$)$_2$(H$_2$bta^{2-}) (**3**)	(4-Br-Hstb$^+$)$_2$(H$_2$bta^{2-}) (**4**)	(3-CN-Hstb$^+$)$_2$(H$_2$bta^{2-}) (**5**)	(2-CN-Hstb$^+$)$_2$(H$_2$bta^{2-}) (**6**)
Chemical formula	$C_{36}H_{26}Cl_2N_2O_8$	$C_{36}H_{24}Cl_4N_2O_8$	$C_{36}H_{26}Br_2N_2O_8$	$C_{36}H_{26}Br_2N_2O_8$	$C_{38}H_{26}N_4O_8$	$C_{38}H_{26}N_4O_8$
Formula weight	685.49	754.37	774.41	774.41	666.63	666.63
Crystal system	Triclinic	Triclinic	Triclinic	Triclinic	Triclinic	Monoclinic
Space group	$P\bar{1}$ (no. 2)	$P\bar{1}$ (no. 2)	$P\bar{1}$ (no. 2)	$P\bar{1}$ (no. 2)	$P\bar{1}$ (no. 2)	$P2_1/c$ (no. 14)
a (Å)	7.466(2)	7.505(2)	7.873(2)	7.413(2)	7.946(2)	13.513(3)
b (Å)	10.993(2)	9.682(2)	9.936(2)	10.094(2)	9.163(2)	6.434(1)
c (Å)	11.026(2)	12.452(3)	11.490(2)	12.181(2)	11.719(2)	18.566(4)
α (°)	111.90(3)	69.07(3)	106.03(3)	113.45(3)	101.68(3)	90
β (°)	95.16(3)	79.63(3)	108.74(3)	99.10(3)	102.13(3)	101.85(3)
γ (°)	108.53(3)	77.91(3)	96.25(3)	101.00(3)	97.57(3)	90
V (Å^3), Z	773.4(3), 1	820.9(3), 1	798.6(3), 1	792.6(3), 1	803.3(3), 1	1579.8(5), 2
dx (g cm^{-3})	1.472	1.526	1.610	1.622	1.378	1.401
F(000)	354	386	390	390	346	692
μ (mm^{-1})	0.27	0.42	2.60	2.62	0.09	0.100
θ range (°)	1.9–27.7	1.8–27.9	1.9–27.9	1.9–27.9	1.8–27.7	3.07–55.50
Reflections collected	9940	10 192	9943	8668	9832	18 641
Reflections unique (R_{int})	3034	3130	3049	2999	3058	3094
Reflections with $I > 2\sigma(I)$	1806	2609	2162	2160	1972	2227
Number of parameters	217	226	217	217	226	221
$R(F^2)$ [$I > 2\sigma(I)$]	0.080	0.047	0.050	0.043	0.089	0.057
w$R(F^2)$ [$I > 2r(I)$]	0.222	0.127	0.139	0.119	0.272	0.155
Goodness of fit on F^2	1.07	1.08	1.06	1.05	1.03	1.08
Max/min $\Delta\rho$ (e Å^{-3})	0.40–0.34	0.19–0.29	0.38–0.52	0.39–0.71	0.88–0.35	0.23–0.20

	(2-Cl-Hstb$^+$)$_2$(H$_2$bta^{2-}) (**7**)	(2-Cl-Hstb$^+$)$_2$ (H$_2$bta^{2-}) (**8**)	(3-Cl-Hstb$^+$)$_2$(H$_2$bta^{2-}) (**9**)	(4-CN-Hstb$^+$)$_2$(H$_2$bta^{2-}) (**10**)	Dimer of 4-CN-stb (**11**)
Chemical formula	$C_{36}H_{26}Cl_2N_2O_8$	$C_{18}H_{13}ClNO4$	$C_{36}H_{26}Cl_2N_2O_8$	$C_{36}H_{26}N_2O_8$	$C_{28}H_{20}N_4$
Formula weight	685.49	342.74	685.49	666.63	412.48
Crystal system	Triclinic	Monoclinic	Monoclinic	Monoclinic	Monoclinic
Space group	$P\bar{1}$ (no. 2)	$P2_1/c1$ (no. 14)	$P2_1/c$ (no. 14)	$P2_1/c$ (no. 14)	$P2_1/c$ (no. 14)
a (Å)	8.918(2)	9.655(2)	9.773(2)	8.812(2)	8.141(2)
b (Å)	9.748(2)	12.927(3)	10.033(2)	11.811(2)	11.929(2)
c (Å)	10.094(2)	13.746(5)	16.112(3)	15.299(5)	11.410(2)
α (°)	64.40(3)	90	90	90	90
β (°)	89.60(3)	114.53(2)	97.83(3)	107.37(3)	107.94(3)
γ (°)	88.69(3)	90	90	90	90
V (Å^3), Z	791.1(3), 1	1560.8(7), 4	1565.1(5), 2	1519.6(6), 2	1054.2(4), 2
dx (g cm^{-3})	1.439	1.454	1.455	1.457	1.299
F(000)	354	708	708	692	432
μ (mm^{-1})	0.264	0.267	0.27	0.104	0.078
θ range (°)	4.57–56.32	4.53–56.22	2.1–27.9	1.72–27.96	2.50–27.28
Reflections collected	9839	19 264	19 945	17 995	11 710
Reflections unique(R_{int})	3033	3041	3202	3133	2178
Reflections With $I > 2\sigma(I)$	2320	1802	2435	2168	889
Number of parameters	217	217	218	226	145
$R(F^2)$ [$I > 2r(I)$]	0.061	0.071	0.051	0.071	0.098
w$R(F^2)$ [$I > 2r(I)$]	0.157	0.189	0.129	0.187	0.222
Goodness of fit on F^2	1.10	1.10	1.08	1.08	1.14
Max/min $\Delta\rho$ (e Å^{-3})	0.45–0.42	0.26–0.44	0.18–0.38	0.25–0.30	0.20–0.20

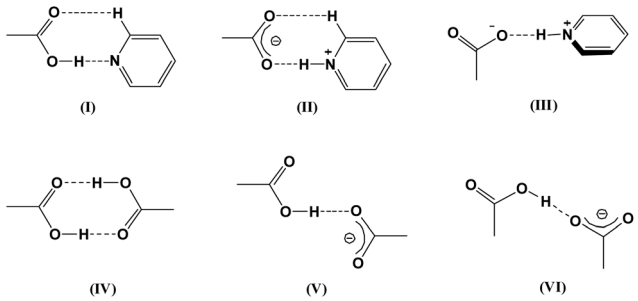

Scheme 3 Schematic representation of different hydrogen bonding synthons: carboxylic-pyridine heterosynthons (I), carboxylate-pyridinium heterosynthons (II and III), centrosymmetric carboxylic acid dimers (IV), and *syn–syn* and *anti–anti* carboxylate–carboxylic interactions (V and VI).

Br-Hstb$^+$)$_2$ (H_2bta^{2-}) (**3**) a structural variant is observed (Fig. 1 (b and c)), where the formation of a double chain between anions and cations is formed by secondary supramolecular interactions (C–H···Cl: 2.832(9) Å) for 4-chloro substitution in structure **2** and C–H···O: 3.424(4) Å in (**3**). Structures (4-Br-Hstb$^+$)$_2$(H_2bta^{2-}) (**4**) and (3-CN-Hstb$^+$)$_2$(H_2bta^{2-}) (**5**) feature additional cation···cation supramolecular interactions: in **4** ternary assemblies are connected *via* Br···Br interactions[15] with a distance of 3.374(2) Å (Fig. 1(d)), and in the case of **5** complementary centrosymmetric CN···H–C: interactions (3.508(2) Å) are observed (Fig. 1(e)).[8a]

In these structures parallel ribbons are stacked in layers and stabilised by π···π interactions. Adjacent layers are connected by complementary multiple C–H···O interactions. Additional C–H···Cl contacts are present in structure **1** through the chlorine atoms in position 2 in the aryl rings. Likewise, in structure **3** we see side-to-side Br···Br interactions between the bromine atoms in ring-position 3, similar to that observed in structure **4** (Br···Br: 3.836(9) Å). In all the structures, such interactions determine the pairwise intercalation of (4-Hstb)$^+$ between the anions stabilised by additional cation–π interactions (Fig. 1(a–e)). This interaction mode leads

Table 2 Hydrogen bond geometry of selected H-bond interactions

Compound	D–H···A	D–H (Å)	H···A (Å)	D···A (Å)	D–H···A (°)
(**1**)	N1–H1N···O3^{i}	0.90	1.80	2.697(5)	172
	N1–H1N···O4^{i}	0.90	2.52	3.184 (5)	131
	Intra O2–H2···O4	1.09	1.37	2.425(5)	160
Symmetry codes: $i = 1 - x, 1 - y, -z$					
(**2**)	N1–H1N···O4^{ii}	0.90	1.73	2.620(3)	171
	Intra O1–H1O···O3	1.13	1.32	2.435(3)	169
Symmetry codes: $ii = -1 + x, y, 1 + z$					
(**3**)	N1–H1N···O4^{iii}	0.90	1.74	2.634(4)	171
	Intra O1–H1O···O3	0.85	1.59	2.433(4)	174
Symmetry codes: $iii = 1 - x, 1 - y, 1 - z$					
(**4**)	N1–H1N···O4^{iv}	0.90	1.80	2.685(4)	166
	Intra O1–H10···O3	1.12	1.30	2.405(4)	170
Symmetry codes: $iv = -x, -y, -z$					
(**5**)	N1–H1N···O1^{v}	0.90	1.82	2.715(4)	174
	Intra O2–H2O···O3	1.04	1.36	2.391(4)	172
Symmetry codes: $v = 1 - x, 1 - y, 2 - z$					
(**6**)	O2–H2O···O4^{vi}	1.04	1.58	2.608(3)	168
	N1–H1N···O3^{vii}	0.90	1.80	2.698(3)	173
Symmetry codes: $vi = -x, 1 - y, -z$; $vii = 1 + x, -1 + y, z$					
(**7**)	N1–H1N···O2^{viii}	0.90	1.71	2.596(4)	168
	O3–H2O···O1^{ix}	0.85	1.76	2.603(3)	175
Symmetry codes: $viii = -x, 1 - y, 1 - z$; $ix = -x, -y, 1 - z$					
(**8**)	N1–H1A···O3^{xi}	0.91	1.99	2.755(5)	151
	O1–H2O···O4^{xii}	0.85	1.41	2.461(4)	158
Symmetry codes: $xi = 1 - x, -y, -z$, $xii = -x, 1/2 + y, 1/2 - z$					
(**9**)	N1–H1N···O2^{xiii}	0.96	1.67	2.621(2)	168
	O3–H1O···O1^{xiv}	0.85	1.63	2.480(2)	173
Symmetry codes: $xiii = 1 + x, 1/2 - y, -1/2 + z$; $xiv = x, 1/2 - y, -1/2 + z$					
(**10**)	N1–H1N···O3^{xv}	0.90	1.77	2.601(4)	152
	O2–H2O···O4^{xvi}	0.85	1.71	2.547(3)	168
Symmetry codes: $xv = x, 1/2 - y, 1/2 + z$; $xvi = 1 - x, 1/2 + y, 1/2 - z$					

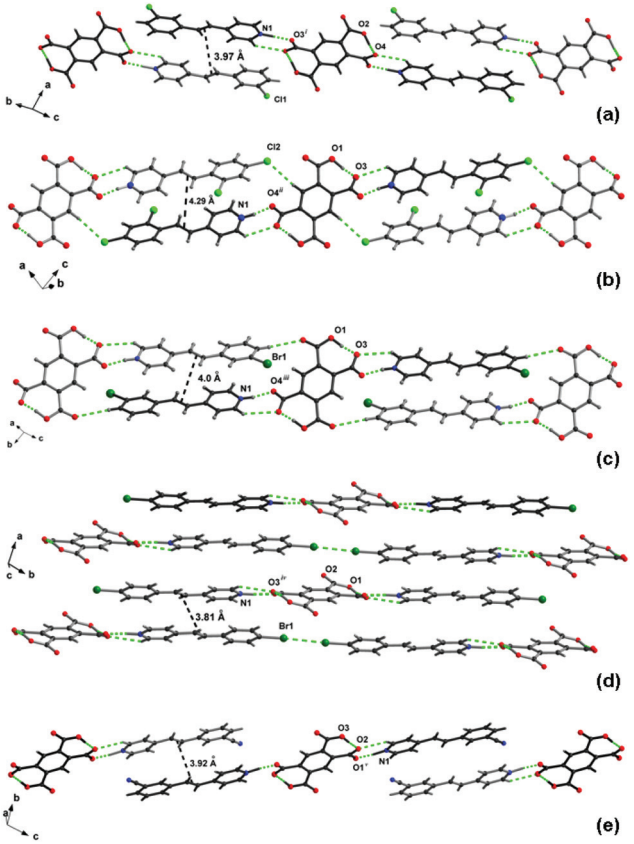

Fig. 1 (a–e) View of the H-bonded ribbons found in the crystal structures of **1–5**. Basic building unit in each structure is highlighted (dark ball and sticks), showing O–H···O$^-$ and N$^+$–H···O$^-$ charge-assisted hydrogen bonds and short contact between double bonds of neighbouring pairs of stilbazolium cations. The Br···Br interactions are indicated for structure of **4** (d). Symmetry codes: *i* = 1 – *x*, 1 – *y*, –*z*; *ii* = –1 + *x*, *y*, 1 + *z*; *iii* = 1 – *x*, 1 – *y*, 1 – *z*; *iv* = –*x*, –*y*, –*z*; *v* = 1 – *x*, 1 – *y*, 2 – *z*.

to face-to-face contacts between adjacent cations, which are oriented in a *head-to-tail* fashion with short contacts between the double bonds of adjacent molecules ≤4.2 Å. Such contacts are suitable for undergoing [2 + 2] cycloaddition reactions in the solid state according to Schmidt's criteria.[16]

Formation of 1-D hydrogen ribbons directed by O–H···O$^-$ and N$^+$–H···O$^-$ charge-assisted hydrogen bonds. Crystal structure of the ionic assembly 6

The crystal structure of (2-CN-Hstb$^+$)$_2$(H$_2$bta^{2-}) (**6**) also forms a ternary ionic from the self-assembly of one H$_2$bta^{2-} dianion and two stilbazolium cations *via* a charge-assisted heterosynthon similar to those observed for structures **1–5** [N1···O1: 2.694(3) Å] Nevertheless, the interaction between the supramolecular motifs is not directed by cation–π interactions (Fig. 2(a)). In the dianion, the carboxylate groups are slightly tilted (15.5°) with respect to the aromatic ring, whereas the carboxylic acid groups are nearly perpendicular to the carboxylate groups. This disposition leads to intermolecular interactions between the carboxylate and carboxylic groups *via* centrosymmetric O–H···O$^-$ H-bonds described by the graph set

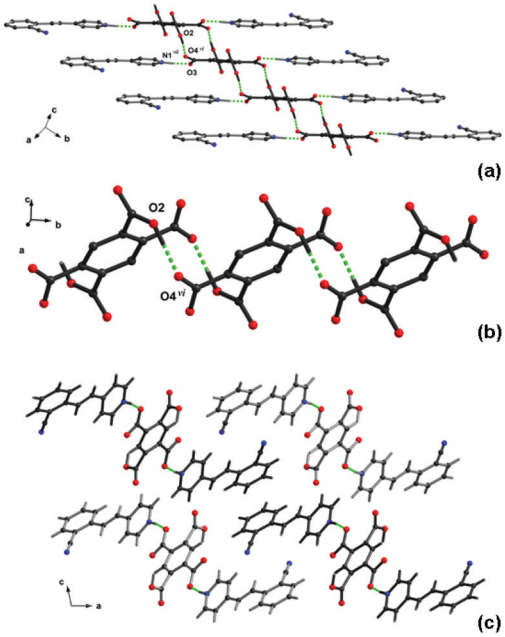

Fig. 2 (a) View of the H-bonded array between found in the crystal structure of **6**. Hydrogen atoms were omitted for clarity, except the involved in H-bonding interactions. (b) *anti–anti* H-bonded ribbons composed of H$_2$bta^{2-} dianion self-assembled *via* carboxylate–carboxylic interactions. (c) View of the stacking of H-bonded ribbons in the *ac*-plane. Symmetry codes: *vi* = –*x*, 1 – *y*, –*z*; *vii* = 1 + *x*, –1 + *y*, *z*.

R$_2^2$(14), contrarily to the formation of intramolecular H-bonds as observed in the previous structures [O2···O4: 2.608(2) Å]. The proton of the carboxylic acid group in the dianion adopts an antiplanar configuration,[17–19] forming zigzag H-bonded ribbons along the *b*-axis (Fig. 2(b)). This interaction mode precludes a *head-to-tail* stacking between the cations as those observed in structures **1–5**. The cations are aligned *head-to-head* to each side of the ribbons in stair-steps fashion along the *c*-axis. These chains are self-assembled *via* cation–cation interdigitation in the *ac*-plane (Fig. 2(c)). This supramolecular organisation does not allow for close contacts between the double bonds, the shortest measuring 6.4 Å

Formation of 2-D hydrogen networks directed by O–H···O$^-$ and N$^+$–H···O$^-$ charge-assisted hydrogen bonds. Crystal structure of the ionic assembly 7

A second 1-D hydrogen bonded array is also observed for structure 2(2-Cl-Hstb$^+$)(H$_2$bta^{2-}) (**7**) (Fig. 3). A comparative analysis with the 1-D hydrogen ribbons found in **6** reveals remarkable structural differences, for example: the connectivity between the dianions in **6** and **7** is different. As in structure **6**, these 1-D ribbons are formed through the same kind of complementary O–H···O$^-$ H-bonds described by the graph notation R$_2^2$(14) between centrosymmetric pairs of carboxylate and carboxylic groups along the *a*-axis [O1···O3: 2.602(3) Å]. However, the relative orientation of the acidic protons in the structure of **7** is planar,[17] in contrast to their antiplanar orientation found in the structure of **6** (Fig. 2(b)). The carboxylate and carboxylic

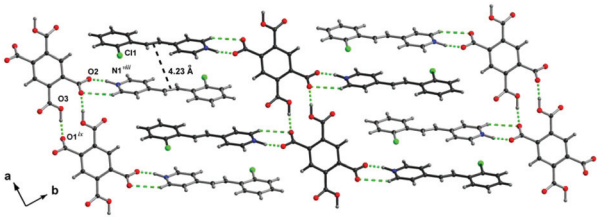

Fig. 3 View of 2D H-bonded network found in the crystal structure of **7**, showing charge-assisted H-bonds cation–anion and *syn–syn* anion–anion H-bonding interactions. Symmetry codes: *viii* = –*x*, 1 – *y*, 1 – *z*; *ix* = –*x*, –*y*, 1 – *z*.

acid groups are twisted by 56.5° and 40.5° with respect to the mean plane of the aromatic ring. Neighbouring H-bonded ribbons are assembled through π–π interdigitation between $(2Cl\text{-}Hstb)^+$ cations linked *via* N^+–H···O^- H-bonds (type II), in a head-to-tail fashion and reinforced through remaining cation–π interactions. These H-bonding interactions interconnect a 2-D H-bonded network parallel to the *ac*-plane. The resulting organisation allows for shorter C═C···C═C contacts (centroid-to-centroid: 4.23 Å) of the pairs of molecules sustained by charge-assisted H-bonds, which is a the borderline value according to the criteria proposed by Schmidt (<4.2 Å).[16]

Formation of 3-D hydrogen networks directed by O–H···O^- and N^+–H···O^- charge-assisted hydrogen bonds. Crystal structures of ionic assemblies 8–10

The crystal structures of $(2\text{-}Cl\text{-}Hstb^+)_2(H_2bta^{2-})$ (**8**), $(3\text{-}Cl\text{-}Hstb^+)_2$ (H_2bta^{2-}) (**9**) and $(4\text{-}CN\text{-}Hstb^+)_2(H_2bta^{2-})$ (**10**) are shown in Fig. 4(b–d). In these structures a novel hydrogen bonding pattern was found. The H_2bta^{2-} anions are self-assembled into square layers *via* H-bonds between carboxylic and carboxylate groups in a *syn–syn* fashion (Fig. 4(a)).[17,19] The carboxylate and carboxylic acid groups are twisted by 73.7° and 6.6° for **8**, 32.3° and 58.1° for **9** and 5.1° and 88.3° for **10** with respect to the mean plane of the aromatic ring. Adjacent layers are connected through $(4\text{-}Hstb)^+$ cations *via* charge-assisted carboxylate–pyridinium supramolecular moieties (Fig. 4(b–d)). Nevertheless, a new supramolecular interaction motif was observed (Type-III), in contrast to the structures described above (Details of geometrical parameters of charge-assisted H-bonds are shown in Table 2). The cations are stacked in a *head-to-tail* fashion directed by cation–π interactions, thus generating a 3-D hydrogen bonded network. In these structures close C═C···C═C contacts are observed (centroid-to-centroid: in the range of 3.9–4.4 Å). Particularly, in structures **8** and **9** these distances are longer than those observed in structures **1–5**, and are slightly over the limit proposed by Schmidt (<4.2 Å).[16]

Supramolecular isomerism

The combination of halogen substituted stilbazoles, such as 2-Cl-4-Stb and 3-Cl-4-Stb, with H_4bta produces two different self-assembled supramolecular organisations *via* O–H···O^- and N^+–H···O^- charge-assisted hydrogen bonds. An analysis of

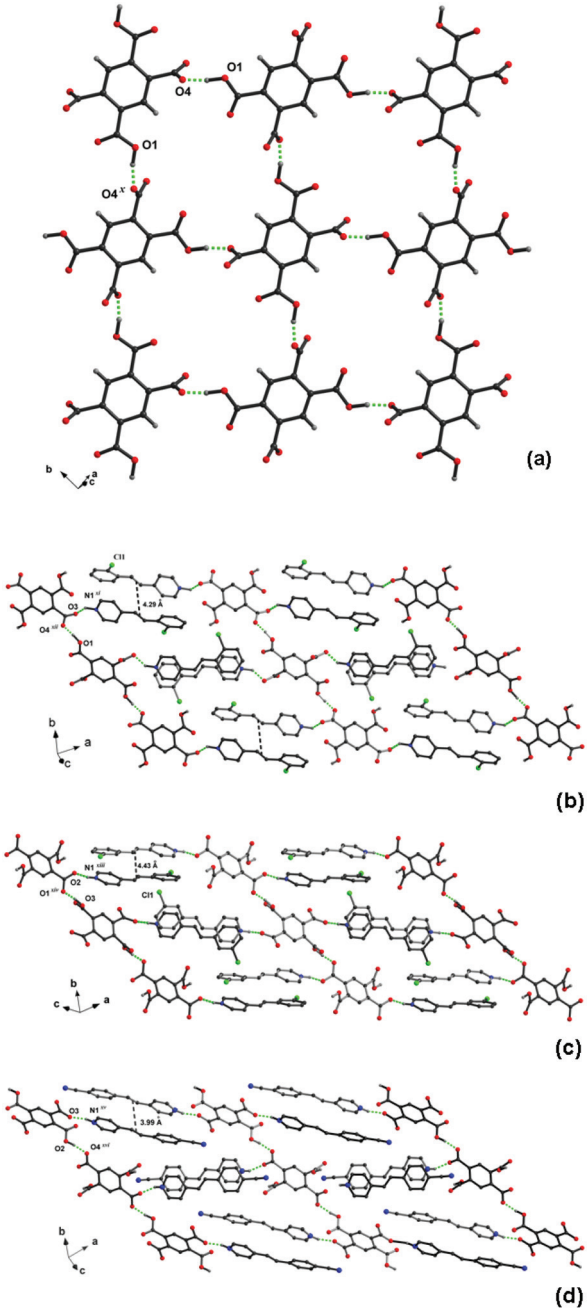

Fig. 4 (a) Schematic representation of 2-D H-bonded network formed *via syn–syn* charge-assisted H-bonds between H_2bta^{2-} anions found for the structures **8–10**. (b–d) Perspective view of 3D crystal structures for the structures **8–10**, showing cation–anion interactions between 2D H-bonded layers *via* charge-assisted carboxylate-pyridinium H-bonding synthons (III) and short contacts between double bonds of the olefins. Symmetry codes: *xi* = 1 – *x*, –*y*, –*z*; *xii* = –*x*, 1/2 + *y*, 1/2 – *z*; *xiii* = 1 + *x*, 1/2 – *y*, –1/2 + *z*; *xiv* = *x*, 1/2 – *y*, –1/2 + *z*; *xv* = *x*, 1/2 – *y*, 1/2 + *z*; *xvi* = 1 – *x*, 1/2 + *y*, 1/2 – *z*.

the factors that affect the preferential formation of each of the observed supramolecular isomers revealed that the selectivity in the crystallisation process is highly dependent on the solvent used. When methanol is used in the case of 2-Cl-4-Stb phase **7** is obtained. However, a methanol–DMSO mixture in a

1 : 1 vol/vol ratio leads to the arrangement **8**. It is worth nothing that the crystallisation is much faster with methanol than with the methanol–DMSO mixture. These results suggest that the formation of the isomers is controlled by kinetic *vs.* thermodynamic factors. Similar structural diversity was obtained with 3-Cl-4-Stb, and crystallisation in methanol leads to the discrete phase **1**, whereas by using a methanol–DMSO mixture the 3D H-bonded network **9** is obtained.

The powder X-ray diffraction patterns match experimental and calculated patterns for polymorphs **1** and **9** together with **7** and **8**, as displayed in Fig. S17 and S24, ESI.† Surprisingly, the PXRD patterns for both pairs of polymorphs are similar, showing only the presence of a single polymorph corresponding to **9**. No additional diffraction peaks are found, even when were identified the corresponding single crystals of **1** and **9** in each case, respectively. It is worth nothing the presence of background radiation in PXRD for **1**, which suggested the possible formation of amorphous material. This could be attributed to the potential transformation of **1** into **9** upon grinding of the sample. Similar transformations have been reported by us and Jones at short grinding times (1–5 min).[9c,10c] We speculate that the ability of different polymorphs to interconvert can provide qualitative information on their crystal structure stabilities. A plausible mechanism would imply the change of an intramolecular to intermolecular H-bond between H_2bta^{2-} anions and re-stacking of stilbazole molecules. In contrast to those polymorphs **7** and **8**, the solids never were obtained as a crystalline single phase with a reasonable structural purity. In both patterns the predominant phase was identified as compound **8** with additional diffraction peaks, which were assigned to the formation of a common crystalline photoproduct based on a further ^{1}H-NMR spectroscopy analyses, where both solids resulted to be photoreactive induced by ambient radiation light. At this point, it was not possible to establish which were the precursor photoactive phases (**7**, **8** or both). Thus, 3D H-bonding networks those observed for **8** and **9** would seem more stable than 1D and 2D H-bonding arrays those found for **1** and **7**, respectively. Although the dimensionality is different in each isomer **7** and **8** of $(2\text{-Cl-4-Stb}^+)_2(H_2bta^{2-})$, the stacking of the cations occurs in a *head-to-tail* fashion with distances C═C···C═C distances (centroid-to-centroid) very near the limit proposed by Schmidt (~4.2 Å). On the contrary, isomers **1** and **9** bearing the (3-Cl-4-Hstb$^+$) cation display notably different C═C···C═C distances of 3.97 Å and 4.42 Å, respectively.

Solid state reactivity studies

Powdered crystalline samples (80 mg) and crystals of **1–10** were irradiated at 302 nm for 2–3 days. The irradiated samples were characterised by ^{1}H-NMR spectroscopy for monitoring the respective topochemical transformations. These photodimers were isolated by extraction with CH_2Cl_2 after neutralization of the acid component with NaOH. During exposure to UV light observation of the irradiated crystals by optical microscopy of compounds **1–10** revealed evident changes in their shapes and colours. The crystals showed a gradual formation of anisotropic internal cracks and fractures on defined faces of the crystal. These changes are associated with movements of the stilbazolium cations located on the potentially reactive planes where dimerisation should occur. Such structural changes suggest that the photoreaction in these cases does not proceed *via* single crystal to single crystal transformation.[20] All compounds were photoreactive with the exception of **6**. Inclusive compound **9** proved to be reactive in spite of displaying larger contacts between double bonds (4.42 Å) compared to the rest of the structures. Similar examples of photoactive crystalline phases with distances in the range 4.2–4.7 Å have been reported recently.[21] The degrees of conversion of the photoactive compounds **1–5** and **7–10** were estimated from ^{1}H NMR spectra.

As expected from crystal structure analyses, the ^{1}H NMR characterisation of the compounds isolated from the irradiated solids confirmed the photodimerisation in the photoactive crystalline phases (Fig. S10–S16†). The spectra of the crude products obtained from **1–10** revealed a high to moderate degrees of conversion. The yields of the photoreactions are summarised in Table 3. All spectra showed the relative decrease or complete disappearance of the signals related to the olefinic protons of starting olefins. Additionally, the appearance of two new peaks in the form of doublets in the range of 4.89–4.53 ppm is characteristic of the C–H protons of a cyclobutane ring with a *rctt*-head to-tail configuration. The chemical shifts of the remaining signals were consistent with the reported ^{1}H NMR pattern of derivatives with such configurations.[1g,6a] In all spectra the presence of only two signals in the region of the aliphatic methine protons revealed the regio- and stereospecific nature of each photoreaction. Several attempts to obtain single crystals of the different photoproducts were unsuccessful with the exception of the photoproduct from the assembly **10**. Finally, the *rctt-head-to tail* stereochemistry of **11** was confirmed by single crystal X-ray diffraction analysis of a sample of the isolated product obtained by recrystallisation from chloroform. The asymmetric unit contains half molecule lies about an inversion centre. The cyclobutane ring adopts a perfectly planar conformation (Fig. 5).

Table 3 Product obtained upon irradiation from the different ionic assemblies. The percentage of conversion (%) was calculated based on integration of ^{1}H NMR signals. Yield of the photoreaction from the assemblies using additional grinding-irradiation cycle

Stilbazolium assembly	C═C··· C═C distance (Å)	H-Bonded array	Yield (%)
(3-Cl-HStb$^+$) (**1**)	3.97	0-D	90
(2,4-di-Cl-HStb$^+$) (**2**)	4.29	0-D	91
(3-Br-HStb$^+$) (**3**)	4.00	0-D	86
(4-Br-HStb$^+$) (**4**)	3.81	0-D	98
(3-CN-HStb$^+$) (**5**)	3.92	0-D	100
(2-CN-HStb$^+$) (**6**)	6.40	1-D	Photoinert
(2-Cl-HStb$^+$) (**7**)	4.23	2-D	83
(2-Cl-HStb$^+$) (**8**)	4.29	3-D	85
(3-Cl-HStb$^+$) (**9**)	4.43	3-D	86
(4-CN-HStb$^+$) (**10**)	3.99	3-D	100

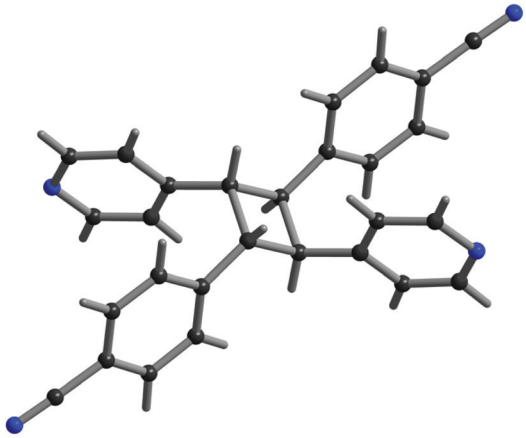

Fig. 5 Ball and stick representation of *rctt*-1,3-bis(4-benzonitrile)-2,4-bis(4-pyridyl)cyclobutane.

Taking advantage of our studies on mechanochemistry in order to improve the yield of any photoreaction *via* multiple grinding-irradiation cycles prompted us to apply a second grinding-irradiation cycle to the remaining irradiated portion.[9c,d,22,23] These mixtures were ground during 15–30 min with some drops of methanol. The resulting mixtures were irradiated again at the same wavelength during the same time periods. ^{1}H-NMR characterization of the extracted solids revealed that the yield of the photodimerisation reactions was always higher than the first set of reactions from one single irradiation cycle (see Table 3), leading to a remarkable improvement of the yields (in some cases nearly to quantitative).

Conclusions

In summary, it has been shown that the use of ionic interactions based on charge-assisted H-bond synthons provides a reliable and directional means to induce self-assembly of organic building blocks into multi-component supramolecular arrays, bearing the adequate geometrical parameters needed for the solid-state photoreactivity from unsaturated targets. We have demonstrated the potential of H_4bta as a useful multivalent H-bonding template to direct synthesis of regio- and stereoselective [2 + 2] photoreactions in the solid state. This molecule acts as an efficient H-bonding supramolecular switch[18,24] to mediate exclusively *head-to-tail* cyclobutanes derived from different stilbazole derivatives, in contrast to homotopic templates. Supramolecular arrays are dominated by the versatility of the H_2bta^{2-} anion to form different self-assemblies *via* O–H···O$^-$ and N$^+$–H···O$^-$ H-bond interactions (Types II, III, V and VI). Besides the *head-to-tail* arrangement, the stacking of the cations is also reinforced by ionic cation–π interactions. This arrangement persists in spite of the presence of distinctive substituents able to direct *head-to-head* arrays, as is the case of –Cl and –Br atoms on the aryl ring by means of attractive halogen···halogen interactions.[15] Such interactions were only observed *via* side interactions through compounds **1–4**. This flexibility of supramolecular interactions allows for a great tolerance either to steric or electronic effects exerted by functional groups in varying numbers and positions, which in some cases leads to polymorphism. Two new examples of supramolecular isomers (**1**, **9**) and (**7–8**) with similar solid state reactivity patterns are disclosed.[3a] In addition, mechanochemical assistance incorporating an additional grinding-irradiation cycle is shown to improve the yield of [2 + 2] photoreactions in the solid state, and this aspect is currently being investigated in our laboratories.

Conflicts of interest

There are no conflicts to declare.

Acknowledgements

We thank FONACIT (grant LAB-97000821) for partial financial support. Lic. D. Briceño (NMR laboratory, IVIC). Profs. G. Díaz de Delgado, J. Contreras (ULA) and E. Ávila (IVIC) for their collaboration with PXRD data collection and analysis.

Notes and references

1 (*a*) Y. Sonoda, Solid-State [2 + 2] Photodimerization and Photopolymerization of α,ω-Diarylpolyene Monomers: Effective Utilization of Noncovalent Intermolecular Interactions in Crystals, *Molecules*, 2011, **16**, 119–148; (*b*) X. Mei, S. Liu and C. Wolf, Template-Controlled Face-to-Face Stacking of Olefinic and Aromatic Carboxylic Acids in the Solid State, *Org. Lett.*, 2007, **9**, 2729–2732; (*c*) A. Papagni, P. Del Buttero, C. Bertarelli, L. Miozzo, M. Moret, M. T. Pryce and S. Rizzato, Novel fluorinated amino-stilbenes and their solid-state photodimerization, *New J. Chem.*, 2010, **34**, 2612–2621; (*d*) B. R. Bhogala, B. Captain, A. Parthasarathy and V. Ramamurthy, Thiourea as a Template for Photodimerization of Azastilbenes, *J. Am. Chem. Soc.*, 2010, **132**, 13434–13442; (*e*) R. C. Grove, S. H. Malehorn, M. E. Breen and K. A. Wheeler, A photoreactive crystalline quasiracemate, *Chem. Commun.*, 2010, **46**, 7322–7324; (*f*) L. R. MacGillivray, Organic Synthesis in the Solid State via Hydrogen-Bond-Driven Self-Assembly, *J. Org. Chem.*, 2008, **73**, 3311–3317; (*g*) L. R. MacGillivray, G. S. Papaefstathiou, T. Friščić, T. D. Hamilton, D.-K. Bučar, Q. Chu, D. B. Varshney and I. G. Georgiev, Supramolecular Control of Reactivity in the Solid State: From Templates to Ladderanes to Metal–Organic Frameworks, *Acc. Chem. Res.*, 2008, **41**, 280–291.

2 (*a*) K. Biradha and R. Santra, Crystal engineering of topochemical solid state reactions, *Chem. Soc. Rev.*, 2013, **42**, 950–967; (*b*) I. G. Georgiev and L. R. MacGillivray, Metal-mediated reactivity in the organic solid state: from self-assembled complexes to metal–organic frameworks, *Chem.*

Soc. Rev., 2007, **36**, 1239–1248; (*c*) J. J. Vittal, Supramolecular structural transformations involving coordination polymers in the solid state, *Coord. Chem. Rev.*, 2007, **251**, 1781–1795; (*d*) M. Nagarathinan, A. M. P. Peedikakkal and J. J. Vittal, Stacking of double bonds for photochemical [2 + 2] cycloaddition reactions in the solid state, *Chem. Commun.*, 2008, 5277–5288; (*e*) D. Liu, N.-Y. Lia and J.-P. Lang, Single-crystal to single-crystal transformation of 1D coordination polymer *via* photochemical [2 + 2] cycloaddition reaction, *Dalton Trans.*, 2011, **40**, 2170–2172; (*f*) I. G. Georgiev, D.-K. Bučar and L. R. MacGillivray, Stereospecific and quantitative photodimerisation of terminal olefins in the solid state, *Chem. Commun.*, 2010, **46**, 4956–4958; (*g*) D. Liu, H. F. Wang, B. F. Abrahams and J. P. Lang, Single-crystal-to-single-crystal transformation of a two-dimensional coordination polymer through highly selective [2 + 2] photodimerization of a conjugated dialkene, *Chem. Commun.*, 2014, **50**, 3173–3175; (*h*) D. Liu and J. P. Lang, Regiospecific photodimerization reactions of an unsymmetrical alkene in two coordination compounds, *CrystEngComm*, 2014, **16**, 76–81.

3 (*a*) A. Briceño, Y. Hill, T. González and G. Díaz de Delgado, Combining hydrogen bonding and metal coordination for controlling topochemical [2 + 2] cycloaddition from multicomponent assemblies, *Dalton Trans.*, 2009, 1602–1610; (*b*) Y. Hill and A. Briceño, Exploiting the use of hydrogen bonding and metal-coordination in the self-assembly of photoreactive multicomponent networks, *Chem. Commun.*, 2007, 3930–3932; (*c*) A. Briceño and A. M. Escalona, Exploiting the use of multivalent interactions in the design of photoreactive supramolecular assemblies. From solution to crystal engineering, in *Photochemistry*, The Royal Society of Chemistry, Cambridge, 2016, vol. 43, pp. 286–320.

4 (*a*) J. N. Gamlin, R. Jones, M. Leibovitch, B. Patrick, J. R. Sheffer and J. Trotter, The Ionic Auxiliary Concept in Solid State Organic Photochemistry, *Acc. Chem. Res.*, 1996, **29**, 203–209; (*b*) Y. Ito, B. Borecka, G. Olovsson, J. Trotter and J. R. Scheffer, Control of the Solid-state photodimerization of some derivatives and analogs of trans-cinnamic acid by ethylenediamine, *Tetrahedron Lett.*, 1995, **36**, 6083–6086.

5 (*a*) S. Yamada and Y. Tokugawa, Cation–π Controlled Solid-State Photodimerization of 4-Azachalcones, *J. Am. Chem. Soc.*, 2009, **131**, 2098–2099; (*b*) S. Yamada, N. Uematsu and K. Yamashita, Role of Cation–π Interactions in the Photodimerization of *trans*-4-Styrylpyridines, *J. Am. Chem. Soc.*, 2007, **129**, 12100–12101; (*c*) S. Yamada, M. Kusafuka and M. Sugawara, [2 + 2] Photodimerization of bispyridylethylenes by a controlled shift of the protonation equilibrium, *Tetrahedron Lett.*, 2013, **54**, 3997–4000.

6 (*a*) B. Mondal, B. Captain and V. Ramamurthy, Photodimerization of HCl salts of azastilbenes in the solid state, *Photochem. Photobiol. Sci.*, 2011, **10**, 891–894; (*b*) M. Pattabiraman, A. Natarajan, R. Kaliappan, J. T. Mague and V. Ramamurthy, Template directed photodimerization of *trans*-1,2-bis(*n*-pyridyl)ethylenes and stilbazoles in water, *Chem. Commun.*, 2005, 4542–4544.

7 (*a*) G. K. Kole, G. K. Tan and J. J. Vittal, Solid state photodimerization of *trans*-2-(4-pyridyl)-4-vinylbenzoic acid *via* salt formation and isomerisation of cyclobutane compounds in solution, *CrystEngComm*, 2012, **14**, 7438–7443; (*b*) G. K. Kole, L. L. Koh, S. Y. Lee, S. S. Lee and J. J. Vittal, A new ligand for metal–organic framework and co-crystal synthesis: mechanochemical route to *rctt*-1,2,3,4-tetrakis-(4′-carboxyphenyl)-cyclobutane, *Chem. Commun.*, 2010, **46**, 3660–3662; (*c*) G. K. Kole, G. K. Tan and J. J. Vittal, Anion-Controlled Stereoselective Synthesis of Cyclobutane Derivatives by Solid-State [2 + 2] Cycloaddition Reaction of the Salts of *trans*-3-(4-Pyridyl) Acrylic Acid, *Org. Lett.*, 2010, **12**, 128–131.

8 (*a*) G. R. Desiraju, Supramolecular Synthons in Crystal Engineering-A New Organic Synthesis, *Angew. Chem., Int. Ed. Engl.*, 1995, **34**, 2311–2327; (*b*) C. B. Aakeröy, A. M. Beatty and B. A. Helfrich, A High-Yielding Supramolecular Reaction, *J. Am. Chem. Soc.*, 2002, **124**, 14425–14432; (*c*) M. D. Ward, Design of crystalline molecular networks with charge-assisted hydrogen bonds, *Chem. Commun.*, 2005, 5838–5842.

9 (*a*) M. Linares and A. Briceño, Solid-state synthesis of head-to-tail photodimers from supramolecular assemblies directed by charge-assisted hydrogen bonds, *New J. Chem.*, 2010, **34**, 587–590; (*b*) A. Briceño and Y. Hill, Exploring the use of anionic homoleptic complexes as templates in the design of photoreactive multi-component supramolecular assemblies, *CrystEngComm*, 2012, **14**, 6121–6125; (*c*) A. Briceño, D. Leal, G. Ortega, G. Díaz de Delgado, E. Ocando and L. Cubillan, Self-assembly, concomitant photochemical processes, and improvement of the yield of [2 + 2] photoreactions from supramolecular arrays *via*, mechanochemical assistance, *CrystEngComm*, 2013, **15**, 2795–2799; (*d*) A. Briceño, D. Leal and G. Díaz de Delgado, A novel example of double reactivity by either photochemical [2 + 2] or thermal additions of an ionic organic supramolecular assembly, *New J. Chem.*, 2015, **39**, 4965–4971.

10 (*a*) N. Shan and W. Jones, Identification of supramolecular templates: design of solid-state photoreactivity using structural similarity, *Tetrahedron Lett.*, 2003, **44**, 3687–3689; (*b*) N. Shan and W. Jones, *Green Chem.*, 2003, **5**, 728; (*c*) S. Karki, T. Friščić and W. Jones, Control and interconversion of cocrystal stoichiometry in grinding: stepwise mechanism for the formation of a hydrogen-bonded cocrystal, *CrystEngComm*, 2009, **11**, 470–481.

11 F. H. Allen, The Cambridge Structural Database: a quarter of a million crystal structures and rising, *Acta Crystallogr., Sect. B: Struct. Sci.*, 2002, **58**, 380–388.

12 B. Moulton and M. J. Zaworotko, From Molecules to Crystal Engineering: Supramolecular Isomerism and Polymorphism in Network Solids, *Chem. Rev.*, 2001, **101**, 1629–1658.

13 G. M. Sheldrick, A short history of SHELX, *Acta Crystallogr., Sect. A: Found. Crystallogr.*, 2008, **64**, 112–122.

14 M. C. Etter, Encoding and decoding hydrogen-bond patterns of organic compounds, *Acc. Chem. Res.*, 1990, **23**, 120–126.

15 (*a*) M. Capdevila-Cortada and J. J. Novoa, The nature of the C–Br···Br–C intermolecular interactions found in molecular crystals: a general theoretical-database study, *CrystEngComm*, 2015, **17**, 3354–3365; (*b*) A. Priimagi, G. Cavallo, P. Metrangolo and G. Resnati, The Halogen Bond in the Design of Functional Supramolecular Materials: Recent Advances, *Acc. Chem. Res.*, 2013, **46**, 2686–2695.

16 G. M. J. Schmidt, Photodimerization in the solid state, *Pure Appl. Chem.*, 1971, **27**, 647–678.

17 L. Leiserowitz, Molecular Packing Modes. Carboxylic Acids, *Acta Crystallogr., Sect. B: Struct. Crystallogr. Cryst. Chem.*, 1976, **32**, 775–802.

18 O. Felix, M. W. Hossini and A. De Cian, Design of 2-D hydrogen bonded molecular networks using pyromellitate dianion and cyclic bisamidinium dication as complementary tectons, *Solid State Sci.*, 2001, **3**, 789–793.

19 J. C. MacDonald, P. C. Dorrestein and M. M. Pilley, Design of Supramolecular Layers via Self-Assembly of Imidazole and Carboxylic Acids, *Cryst. Growth Des.*, 2001, **1**, 29–38.

20 (*a*) T. Friščić and L. R. MacGillivray, Single-crystal-to-single-crystal [2 + 2] photodimerizations: from discovery to design, *Z. Kristallogr. – Cryst. Mater.*, 2009, **220**, 351–363; (*b*) M. A. Garcia-Garibay, Molecular crystals on the move: from single-crystal-to-single-crystal photoreactions to molecular machinery, *Angew. Chem., Int. Ed.*, 2007, **46**, 8945–8947 and references therein.

21 (*a*) K. Tsaggeos, N. Masiera, A. Niwicka, V. Dokorou, M. G. Siskos, S. Shoulika and A. Michaelides, Crystal Structure, Thermal Behavior, and Photochemical Reactivity of a Series of Co-Crystals of *trans*-1,2-Bis(4-pyridyl) Ethylene with Dicarboxylic Acids, *Cryst. Growth Des.*, 2012, **12**, 2187–2194; (*b*) I. Fonseca, M. Baias, S. E. Hayes, C. J. Pickard and M. Bertmer, Size effects of aromatic substitution in the *ortho*position on the photodimerization kinetics of α-*trans*, cinnamic acid derivatives. A solid-state NMR study, *Phys. Chem. Chem. Phys.*, 2009, **11**, 10211–10218.

22 F. Toda, K. Tanaka and A. Sekikawa, Host–guest complex formation by a solid–solid reaction, *J. Chem. Soc., Chem Commun.*, 1987, 279–280.

23 A. N. Sokolov, D.-K. Bučar, J. Baltrusaitis, S. X. Gu and L. R. MacGillivray, Supramolecular catalysis in the organic solid state through dry grinding, *Angew. Chem., Int. Ed.*, 2010, **49**, 4273–4277.

24 (*a*) A. Dey, S. Bera and K. Biradha, Cocrystals and Salts of Pyridine-3,5-bis(1-methyl-benzimidazole-2-yl) with Pyromellitic Acid: Aromatic Guest Inclusion and Separation via Benzimidazole-Carboxylic Acid Heterosynthon, *Cryst. Growth Des.*, 2015, **15**, 318–325; (*b*) O. Fabelo, L. Cañadillas-Delgado, F. S. Delgado, P. Lorenzo-Luis, M. Laz, M. Julve and C. Ruiz-Pérez, Hydrogen Bond-Directed Frameworks Based on 1,2,4,5-Benzene-Tetracarboxylate, *Cryst. Growth Des.*, 2005, **5**, 1163–1167.